DEBRIS FLOWS: Disasters, Risk, Forecast, Protection

Proceedings
of the 7th International Conference

Chengdu, China, 23–27 September 2024

Edited by
S.S. Chernomorets, K. Hu, K.S. Viskhadzhieva

Geomarketing LLC
Moscow
2024

СЕЛЕВЫЕ ПОТОКИ: катастрофы, риск, прогноз, защита

Труды
7-й Международной конференции

Чэнду, Китай, 23–27 сентября 2024 г.

Ответственные редакторы
С.С. Черноморец, К. Ху, К.С. Висхаджиева

ООО «Геомаркетинг»
Москва
2024

泥石流：
灾害、风险、预测、防治

會議記錄
第七届国际会议

中国成都, 2024年9月23日至27日

編輯者
S.S. Chernomorets, K. Hu, K. Viskhadzhieva

Geomarketing LLC
莫斯科
2024

УДК 551.311.8
ББК 26.823
С29

Debris Flows: Disasters, Risk, Forecast, Protection. Proceedings of the 7th International Conference (Chengdu, China). – Ed. by S.S. Chernomorets, K. Hu, K.S. Viskhadzhieva. – Moscow: Geomarketing LLC. 622 p.

Селевые потоки: катастрофы, риск, прогноз, защита. Труды 7-й Международной конференции (Чэнду, Китай). – Отв. ред. С.С. Черноморец, К. Ху, К.С. Висхаджиева. – Москва: ООО «Геомаркетинг», 2024. 622 с.

泥石流：灾害、风险、预测、防治. 會議記錄 第七届国际会议. 中国成都. 編輯者 S.S. Chernomorets, K. Hu, K.S. Viskhadzhieva. – 莫斯科: Geomarketing LLC. 622 p.

ISBN 978-5-6050369-6-8

Ответственные редакторы: С.С. Черноморец (МГУ имени М.В. Ломоносова), К. Ху (Институт горных опасностей и окружающей среды Китайской академии наук), К.С. Висхаджиева (МГУ имени М.В. Ломоносова).

Edited by S.S. Chernomorets (Lomonosov Moscow State University), K. Hu (Institute of Mountain Hazards and Environment, CAS), K.S. Viskhadzhieva (Lomonosov Moscow State University).

При создании логотипа конференции использован рисунок из книги С.М. Флейшмана «Селевые потоки» (Москва: Географгиз, 1951, с. 51).

Conference logo is based on a figure from S.M. Fleishman's book on Debris Flows (Moscow: Geografgiz, 1951, p. 51).

© Селевая ассоциация

© Debris Flow Association

Evaluating earthquake-induced landslide potential under different scenarios using empirical landslide fragility model – A case study on Taiwan

M.H. Hsieh

China University of Technology, Taipei, Taiwan, China, hsiehmh.fcu@gmail.com

Abstract. An earthquake with a magnitude of M_w = 7.0 or greater occurs in Taiwan and its neighboring ocean areas every 2.5 years. Earthquakes may trigger landslides, leading to unstable soil and sand disasters. The study aims to investigate the potential widespread slope landslides that may follow catastrophic earthquakes. The research employs landslide fragility analysis to evaluate the probability and scope of landslides for different earthquake magnitudes. Furthermore, the assessment of slope landslide potential was conducted using the regional slope landslide assessment database, considering 5 distinct scenarios for the protection faults in the study area. The study revealed significant differences in peak ground acceleration (PGA) and peak ground velocity (PGV). In areas with high seismic activity, PGV emerges as a more sensitive and indicative factor of slope landslides. Thus, PGV is deemed more appropriate as an indicator of earthquake-induced landslides, aiding in the identification of high-risk zones post-earthquakes. Moreover, earthquake-induced landslides were notably more frequent following earthquakes of magnitude Mw = 7.5. The findings of this research can be utilized for various disaster prevention purposes and can serve as a valuable resource for earthquake disaster prevention and mitigation strategies in watershed regions.

Key words: *earthquake, landslide fragility, probability model, earthquake magnitude, scenario analysis*

Cite this article: Hsieh M.H. Evaluating earthquake-induced landslide potential under different scenarios using empirical landslide fragility model – A case study on Taiwan. In: Chernomorets S.S., Hu K., Viskhadzhieva K.S. (eds.) Debris Flows: Disasters, Risk, Forecast, Protection. Proceedings of the 7th International Conference (Chengdu, China). Moscow: Geomarketing LLC, 2024, p. 157–165.

Оценка вероятности схода оползней, вызванных землетрясениями, при различных сценариях с использованием эмпирической модели поведения оползней на примере Тайваня

М.С. Сие

Китайский технологический университет, Тайбэй, Тайвань, Китай, hsiehmh.fcu@gmail.com

Аннотация. Землетрясения с магнитудой M_w = 7,0 или выше происходят на Тайване и в соседних районах каждые 2,5 года. Они могут вызывать оползни, что приводит к нестабильности грунтов. Цель исследования – изучить вероятность формирования оползней, которые могут возникнуть после катастрофических землетрясений. Для этого испльзовался анализ поведения оползней для оценки вероятности их схода и масштабов при различных магнитудах землетрясений. Оценка проводилась с использованием региональной базы данных с учетом пяти различных сценариев для разломов в районе исследования. Были выявлены значительные различия в пиковых ускорениях (PGA) и скоростях (PGV) грунта. В районах с высокой сейсмической активностью PGV оказывается более чувствительным и показательным параметром для оползней на склонах, а потому считается более предпочтительным для исследования сейсмогенных оползней и помогает выявлять зоны повышенного

риска после землетрясений. Более того, установлено, что сейсмогенные оползни происходили значительно чаще после землетрясений с магнитудой M_w = 7,5. Результаты данного исследования могут быть использованы в различных целях для предотвращения стихийных бедствий и послужить ценным ресурсом для стратегий предупреждения и смягчения последствий землетрясений в горных регионах.

Ключевые слова: *землетрясение, потенциал оползней, вероятностная модель, магнитуда землетрясения, анализ сценариев*

Ссылка для цитирования: Сие М.С. Оценка вероятности схода оползней, вызванных землетрясениями, при различных сценариях с использованием эмпирической модели поведения оползней на примере Тайваня. В сб.: Селевые потоки: катастрофы, риск, прогноз, защита. Труды 7-й Международной конференции (Чэнду, Китай). – Отв. ред. С.С. Черноморец, К. Ху, К.С. Висхаджиева. – М.: ООО «Геомаркетинг», 2024, с. 157–165.

Introduction

Earthquakes occur frequently in Taiwan due to its location at the convergence of the Philippine Sea and Eurasian plates in a seismically active region. This geographical positioning often leads to severe disasters in mountainous areas. Apart from causing structural damage, strong earthquakes pose a significant risk of slope failure. However, accurately predicting earthquakes using current technology remains a formidable task, and the physical processes that trigger slope failures are highly intricate. Consequently, forecasting, alerting, and assessing the extensive slope hazards directly induced by earthquakes is challenging. The Chi-Chi earthquake on September 21, 1999, with a magnitude of 7.6, activated the Chelongpu faults, destabilizing vulnerable geological formations and resulting in widespread calamities. Given these geohazard complexities, conducting assessments of slope risks is imperative for regions with elevated susceptibility to such hazards.

The analysis of factors that influence landslides triggered by seismic events is notably intricate. Consequently, evaluations of slope hazards associated with earthquakes necessitate the consideration of multiple risk elements. Nevertheless, the complexity and uncertainty stemming from environmental variables, coupled with insufficient data, represent two key limitations impeding the advancement of landslide assessment frameworks [*Ozturk et. al., 2016*]. Traditionally, the evaluation of slope susceptibility relied on models that classified regions based on potential triggers like seismic activity or precipitation [*Dias et. al., 2021; Hodasova and Bednarik, 2021*]. However, empirical post-earthquake studies have revealed instances of diverse geohazards manifesting on slopes with comparable geographical and environmental characteristics. This variability introduces significant uncertainty into slope landslide assessments. Hence, it is imperative to incorporate the diversity of environmental factors into slope vulnerability models to enhance the dependability of assessment outcomes.

This study introduces a methodology for evaluating post-earthquake slope landslides using landslide fragility curves. These curves indicate the probability of landslides occurring after an earthquake and can be applied for landslide assessment and scenario simulation post-earthquake events. The fragility curves are established based on historical data of earthquake-induced landslides, making them more comprehensive, reliable, and realistic for earthquake scenario modeling and evaluation. The research classifies slopes into 12 categories based on key geological factors and utilizes a dataset of 921 earthquakes to develop landslide fragility curves, with PGA and PGV as the triggering factors [*Hsieh et. al., 2023*]. The research employs five earthquake events in Taiwan to replicate post-earthquake landslide scenarios and subsequently compares their characteristics and potential for practical implementation in earthquake assessments. The findings of the research can be utilized for the real-time assessment of prospective seismic occurrences and for scenario modeling in the context of hypothetical earthquakes. As a result, they can serve multiple disaster prevention objectives and provide a basis for earthquake prevention and mitigation strategies in the basin region.

Methods

Landslide fragility analysis

The analysis of landslide fragility is a probabilistic model used for slope risk assessment. It assesses the probability of landslides occurring based on factors such as Peak Ground Acceleration (PGA), Peak Ground Velocity (PGV), Peak Ground Displacement (PGD), and other seismic indicators. Seismologists have assumed that the log-normal distribution of the ground motion factor represents the rate of damage [*Shinozuka et. al., 2000; Hsieh et. al., 2013*]. In this study, the curve representing this distribution is defined by two parameters, the mean (μ) and standard deviation (σ), for a random variable, a. These dual parameters are calculated and then inserted into the cumulative distribution function to determine the probability distribution of earthquake-induced landslides as follows:

$$F_x(a;\mu,\sigma) = \frac{1}{2}\left(1 + erf\left[\frac{\ln a-\mu}{\sigma\sqrt{2}}\right]\right), \quad (1)$$

$F_x(a)$ is the cumulative distribution function of the log-normal distribution, and erf is the Gaussian error function. The parameters (μ, σ) of the fragility function are solved using the MLE method, continuing the work of *Shinozuka et al*., the maximum likelihood function $L(a)$ can be shown as follows:

$$L(a) = \prod_{n=1}^{K}[F(a)]^{x_n} \cdot [1 - F(a)]^{1-x_n}. \quad (2)$$

Here, L(a) is a function of two parameters (μ, σ), where a is a random variable (i.e. seismic indicator), K is the total number of slopes, and the value of x_n is 0 or 1. While a landslides occurred, x_n =1; otherwise, x_n =0. $F(a)$ is the standardized log-normal distribution, as shown as follows:

$$F(a;\mu,\sigma) = \Phi\left[\frac{\ln\left(\frac{a}{\mu}\right)}{\sigma}\right]. \quad (3)$$

To obtain the extreme value of the maximum likelihood function, the two parameters (μ, σ) must satisfy the following equations:

$$\frac{\partial \ln L}{\partial \sigma} = \frac{\partial \ln L}{\partial \mu} = 0. \quad (4)$$

Landslide fragility curves. Slope typologies

The slopes are classified into 12 categories based on their geographic characteristics, such as geology, slope sensitivity, and gradient. Geology, also known as lithology, is divided into two categories: G1 (dense soil and soft rock) and G2 (hard and brittle rock). Slope sensitivity is categorized into two groups: A1 (weak) and A2 (strong). The slope gradient is classified into three categories: S1 (gentle), S2 (medium), and S3 (steep). Each category of slope is characterized by distinct geologic features, which play a role in determining the probability of landslides. Slope sensitivity refers to the susceptibility of the slope surface to collapse, influenced by factors such as the seismic source direction, earthquake wave direction, and slope orientation [*Lin et.al., 2020*].

Fragility curves

Based on the empirical landslide data associated with different slope types during the 921 earthquakes, the dual parameters of the fragility function can be ascertained through Equation (4). The initial phase involves the creation of a seismic event database encompassing

diverse slope categories. Subsequently, utilizing the Maximum Likelihood Estimation (MLE) technique, the median and standard deviation values are computed for each classification cohort. The ultimate outcomes, comprising the mean and standard deviation for individual slope types, are delineated in Tables 1 and 2. These tables present the outcomes concerning PGA and PGV as seismic variables, respectively. The quantity of slope units in the tables denotes the quantity of slopes scrutinized within each slope type of slope database.

Table 1. The dual parameters for 12 groups of slope types for PGA factor

Group number	Number of slope units	Median	Standard deviation	Data range (cm/s^2)	
G1A1S1	261	0.952	0.681	250.00 to	474.48
G1A1S2	131	0.771	0.581	250.00 to	476.34
G1A1S3	116	0.683	0.498	250.00 to	480.94
G1A2S1	262	1.035	0.734	250.00 to	473.17
G1A2S2	67	0.878	0.662	250.00 to	462.68
G1A2S3	63	0.789	0.598	250.00 to	484.24
G2A1S1	1498	0.496	0.128	250.00 to	592.74
G2A1S2	553	0.482	0.118	250.00 to	573.98
G2A1S3	552	0.468	0.112	250.00 to	558.90
G2A2S1	1354	0.525	0.164	250.00 to	601.62
G2A2S2	474	0.521	0.152	250.00 to	595.41
G2A2S3	543	0.518	0.139	250.00 to	585.77

Table 1. The dual parameters for 12 groups of slope types for PGV factor

Group number	Number of slope units	Median	Standard deviation	Data range (cm/s)	
G1A1S1	261	0.836	0.644	50.00 to	88.75
G1A1S2	131	0.700	0.559	50.00 to	94.73
G1A1S3	116	0.573	0.487	50.00 to	101.50
G1A2S1	262	1.061	0.750	50.00 to	88.51
G1A2S2	67	0.926	0.686	50.00 to	92.02
G1A2S3	63	0.855	0.629	50.00 to	102.20
G2A1S1	1498	0.431	0.120	50.00 to	108.59
G2A1S2	553	0.418	0.111	50.00 to	111.87
G2A1S3	552	0.406	0.105	50.00 to	115.67
G2A2S1	1354	0.456	0.154	50.00 to	110.21
G2A2S2	474	0.452	0.143	50.00 to	116.04
G2A2S3	543	0.450	0.131	50.00 to	121.23

The cumulative probability distribution for each slope type can be graphed based on the dual parameters of the 12 typologies of fragility functions. This graphical representation, depicted in Figs. 1 and 2, is commonly referred to as the landslide fragility curve. These curves delineate the probability of landslides occurring on different types of slopes at varying levels of seismic intensity. Within the figures, landslide fragility curves are displayed for four categories of geomorphic factors, categorized by the slope gradient factor, to contrast the probability of landslides under different gradient conditions. The disparity in landslide occurrence rates across different slope types is prominently observable in the figures. Particularly, the discrepancy between geology types G1 and G2 is more pronounced, while the variance in gradient conditions is less notable for the G2 geology type.

Earthquake-induced landslide scenarios

In this study, the changes and effects of post-seismic landslides were discussed at different earthquake magnitudes. Five faults were selected to evaluate the landslide volume in Taiwan: the Shanjiao Fault, the Chelongpu Fault, the Chaozhou Fault, the Chishang Fault, and the Chukou Fault. These five faults are located throughout Taiwan and are representative of the geological characteristics of regional faults. An earthquake with a magnitude of 7.1 to 7.8 was selected for the simulation because the magnitude of earthquake-induced slope failures necessitates a sufficiently strong earthquake.

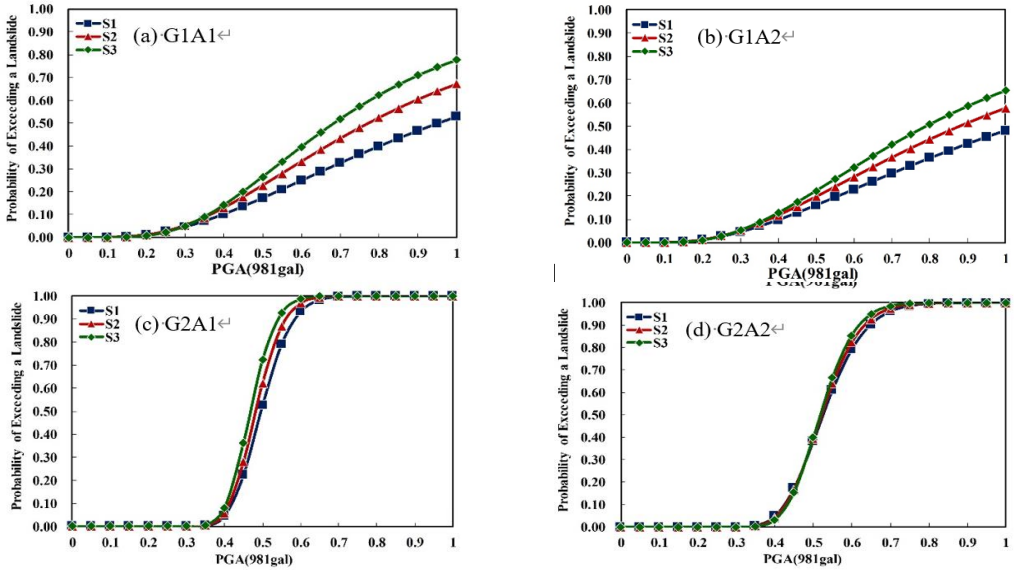

Fig. 1. Landslide fragility curve with (PGA factor) comparison of gradient conditions S1, S2, and S3.

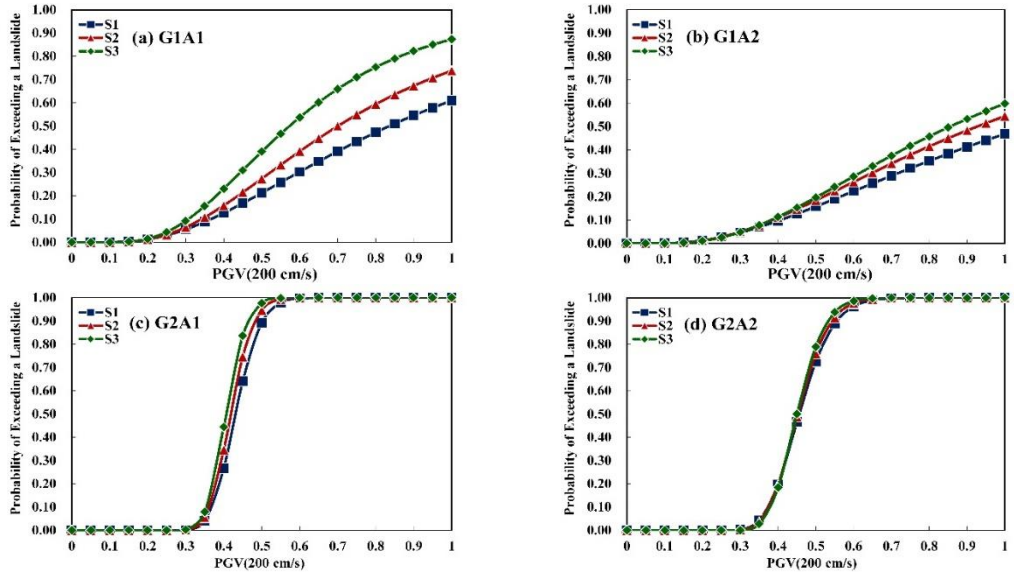

Fig. 2. Landslide fragility curve (PGV factor) comparison of gradient conditions S1, S2, and S3

The slope landslide assessment model utilizes equation (1) to compute the collapse probability value of a specific type of slope under seismic conditions, representing the probability of landslide. In this study, slope landslide is defined as either the failure rate exceeding 5% or the failure extending to a specific horizontal projected area. In such instances, the anticipated collapse loss can be delineated within a defined scope. When the surface seismic

activity surpasses a threshold value (PGA ≥ 250 cm/s2; PGV ≥ 50 cm/s), the minimum achievable collapse area (AL_{min}) for a slope unit is determined.

$$AL_{min} = 0.05 \times A_{su}. \quad (5)$$

In the above equation, A_{su} represents the effective area of the slope unit. The maximum potential collapse area (AL_{max}) is calculated as follows:

$$AL_{max} = \mathrm{V} \times A_{su}. \quad (6)$$

Results and discussion

The results of the landslides assessment with PGA as a factor are shown in Table 3, and the change in landslide area is depicted in Fig. 3 to Fig. 4. Similarly, the results of the collapse assessment with PGV as a factor are presented in Table 4, and the change in landslide area is illustrated in Fig. 5 to Fig. 6. From the table, it can be seen that the landslide area is higher when PGA is the factor, while it is lower when PGV is the factor.

Table 3. The results of PGA as a factor for different earthquake magnitudes

Fault	Shanjiao		Chelongpu		Chaozhou		Chishang		Chukou	
Mag.	Min.	Max.	Min.	Max.	Min.	Max.	Min.	Max.	Min.	Max.
7.1	23	1486	14	3612	54	6260	82	4388	13	2604
7.2	34	1857	22	4623	74	7542	112	5444	19	3161
7.3	50	2335	35	5915	102	8996	155	6718	27	3844
7.4	72	2947	67	7550	143	10682	217	8255	38	4705
7.5	102	3700	110	9602	196	12630	299	10129	53	5753
7.6	135	4610	181	12103	257	14876	409	12383	76	7017
7.7	176	5703	277	15119	338	17375	540	15048	110	8520
7.8	223	6927	410	18703	440	20190	708	18154	153	10257

Unit: hectare.

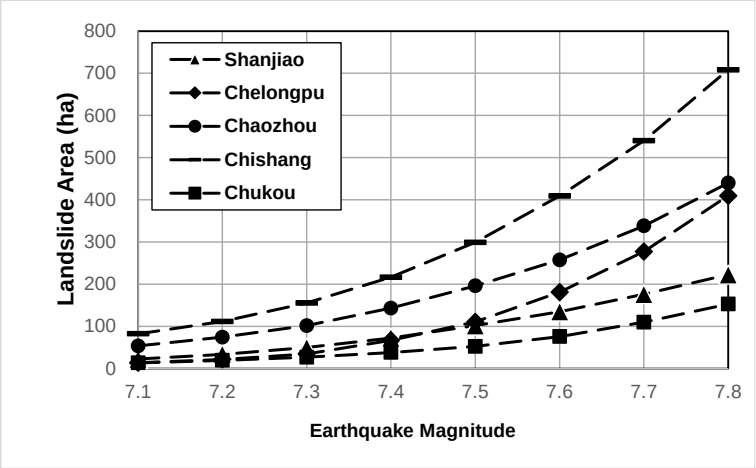

Fig. 3. Minimum landslide area of different magnitudes for PGA factor

For the PGA factor, the minimum landslide area at magnitude 7.1 is less than a hundred hectares, and the maximum landslide area can be several thousand hectares. In contrast, the minimum landslide area at magnitude 7.8 is more than a hundred hectares, and the maximum landslide area is close to 20,000 hectares. Overall, the landslide area increases with the magnitude, and the rate of increase is slower than that of the PGV factor. Specifically, the growth in maximum landslide area is roughly linear. While there are variations in the collapse characteristics of the faults, they typically exhibit similar patterns of increase and trends.

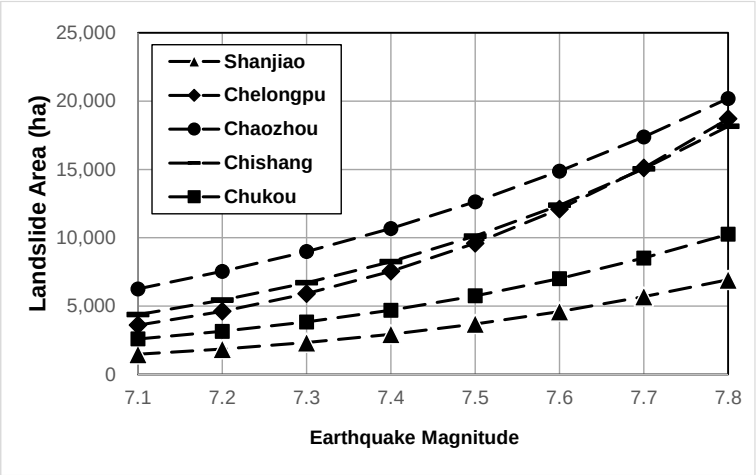

Fig. 4. Maximum landslide area of different magnitudes for PGA factor

Table 4. The results of PGA as a factor for different earthquake magnitudes

Fault	Shanjiao		Chelongpu		Chaozhou		Chishang		Chukou	
Mag.	Min.	Max.	Min.	Max.	Min.	Max.	Min.	Max.	Min.	Max.
7.1	0	259	0	337	0	768	0	389	0	472
7.2	1	351	0	640	1	1588	1	955	0	759
7.3	2	588	1	1299	11	2858	17	1931	2	1222
7.4	6	1067	6	2664	26	4814	47	3473	7	2023
7.5	34	2052	24	5492	70	7827	120	6146	19	3524
7.6	123	3996	169	11227	175	12171	342	10940	67	6272
7.7	282	7155	648	21347	380	18400	825	18899	223	10909
7.8	497	11436	1628	36799	734	26861	1632	30703	521	17944

Unit: hectare.

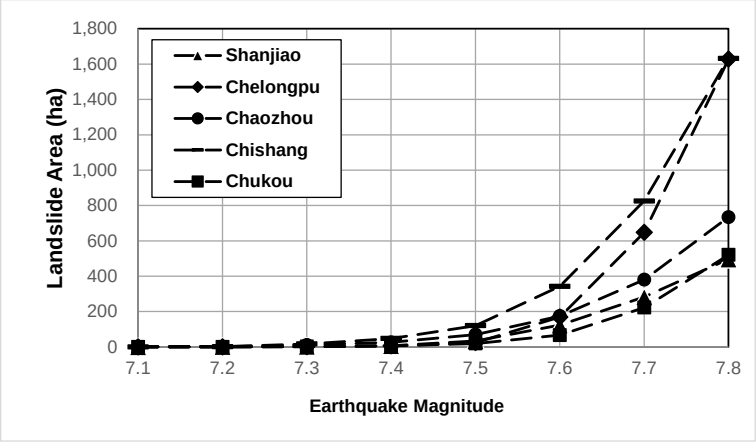

Fig. 5. Minimum landslide area of different magnitudes for PGV factor

For the PGV factor, the minimum landslide area at magnitude 7.1 is almost zero, and the maximum landslide area is under a thousand hectares, while the minimum collapse area at magnitude 7.8 is almost 500 hectares, and the maximum landslide area is close to 37,000 hectares. The area affected by landslides increases sharply and exponentially as the magnitude increases, highlighting the distinction between the PGV factor and the PGA. Similarly, while the collapse characteristics of faults may vary slightly, the magnitude and overall trend are generally similar.

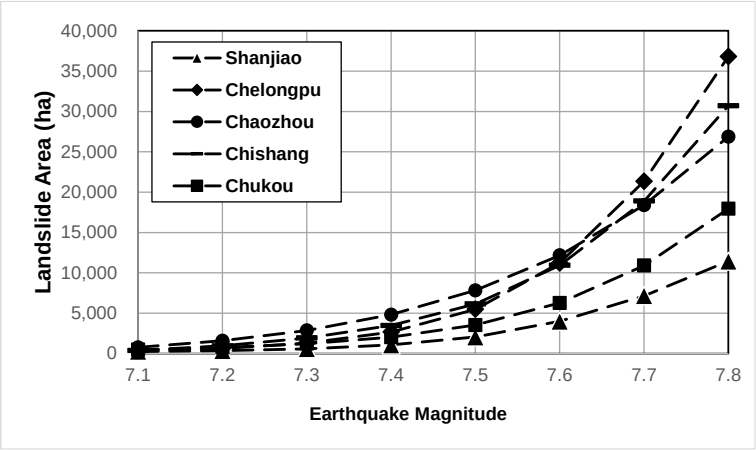

Fig. 6. Maximum landslide area of different magnitudes for PGV factor

In addition, the rate of increase in landslide area is slower before an earthquake magnitude of 7.5 when using PGV as a factor, while larger earthquake magnitudes result in a greater landslide area. This means that using PGV as a seismicity index in high-seismicity regions will better reflect the strong correlation between the magnitude classification and the severity of the actual disaster. In addition, it should be noted that the graphs also indicate that the landslide area of the PGA is higher than that of the PGV for smaller earthquake magnitudes, and vice versa for larger earthquake magnitudes.

Conclusions

Based on the aforementioned analysis of the impacts of earthquakes of varying magnitudes, the following four points can be summarized:

- the assessment of PGA exhibits lower sensitivity compared to PGV in relation to landslide risk associated with different earthquake magnitudes. This is due to the nearly linear outcomes, indicating that the risk of slope failures for varying earthquake magnitudes remains relatively consistent for a given seismic event source. Conversely, PGV demonstrates higher sensitivity, leading to varying risks of slope failure across different earthquake magnitudes;
- based on the data provided by PGV, earthquake magnitudes can be divided into two segments using 7.5 as the threshold. Magnitudes below 7.5 demonstrate a nearly linear pattern, while magnitudes equal to or exceeding 7.5 exhibit a sharp rise. A multinomial fitting approach is employed by aggregating the assessments of individual faults;
- in this study, multinomial fitting was conducted by averaging the outcomes of each cross-sectional evaluation. The minimum landslide area was identified to exhibit four times more curvature, rendering it more responsive in contrast to the maximum landslide area. This highlights the sensitivity of the minimum landslide area that aligns with the landslide definition in this research, emphasizing a clear differentiation among different slope unit categorizations. The maximum landslide area represents a pessimistic approximation that assumes the total collapse of the slope; however, it is, in fact, a highly conservative estimation;
- the findings of the results of PGV analysis, it can be seen that the energy release associated with an escalation in earthquake magnitude results in a notable increase in the projected collapse value. In contrast to the PGA, which assesses the anticipated amplification of gradual collapse, utilizing PGV as a parameter for essential characterization in disaster readiness is deemed more rational and efficient.

Acknowledgements

This study was funded by the Soil and Water Conservation Bureau in Taiwan, with support provided under grant numbers SWCB-111-051 and SWCB-112-062.

References

Dias, H.C., Gramani, M.F., Grohmann, C.H., Bateira, C., Vieira, B.C. (2021). Statistical-based shallow landslide susceptibility assessment for a tropical environment: a case study in the southeastern Brazilian coast. Natural Hazards, 108: 205–223.

Hodasova, K., Bednarik, M. (2021). Effect of using various weighting methods in a process of landslide susceptibility assessment. Natural Hazards, 105: 481–499.

Hsieh, M.H., Lee, B.J., Lei, T.C., Lin, J.Y. (2013). Development empirical fragility curves of RC building based on the Chi–Chi Earthquake data. Nat Hazards 69(1), 695–728.

Hsieh, M.H., Lin, B.S., Lin, L.W. (2023). Development of Earthquake-induced Landslide Fragility Analysis Based on Earthquake Data. Mediterranean Geosciences Union-23, Istanbul, Turkey.

Lin, J.W., Hsieh, M.H., Li, Y.J. (2020). Factor analysis for the statistical modeling of earthquake-induced landslides. Front Struct Civ Eng 14(1), 123–126.

Ozturk, U., Tarakegn, Y.A., Longoni, L., Brambilla, D., Papini, M., Jensen, J. (2016). A simplified early-warning system for imminent landslide prediction based on failure index fragility curves developed through numerical analysis. Geom Nat Hazards Risk 7(4), 1406–1425.

Shinozuka, M., Feng, M.Q., Lee, J., Naganuma, T. (2000). Statistical analysis of fragility curves. Journal of Engineering Mechanics-ASCE, 126(12): 1224–1231.